CHEMISTRY
A EUROPEAN JOURNAL

ChemPubSoc Europe

DOI: 10.1002/chem.201203045

Solid-State Thermolysis of a *fac*-Rhenium(I) Carbonyl Complex with a Redox Non-Innocent Pincer Ligand

Titel Jurca,[a] Wen-Ching Chen,[b] Sheila Michel,[a] Ilia Korobkov,[a] Tiow-Gan Ong,[b] and Darrin S. Richeson*[a]

Abstract: The development of rhenium(I) chemistry has been restricted by the limited structural and electronic variability of the common pseudo-octahedral products *fac*-$[ReX(CO)_3L_2]$ (L_2 = α-diimine). We address this constraint by first preparing the bidentate bis(imino)pyridine complexes [(2,6-{2,6-$Me_2C_6H_3N{=}CPh\}_2C_5H_3N$)$Re(CO)_3$-X] (X = Cl **2**, Br **3**), which were characterized by spectroscopic and X-ray crystallographic means, and then converting these species into tridentate pincer ligand compounds, [(2,6-{2,6-$Me_2C_6H_3N{=}CPh\}_2C_5H_3N$)$Re(CO)_2$X] (X = Cl **4**, Br **5**). This transformation was performed in the solid-state by controlled heating of **2** or **3** above 200 °C in a tube furnace under a flow of nitrogen gas, giving excellent yields (≥95 %). Compounds **4** and **5** define a new coordination environment for rhenium(I) carbonyl chemistry where the metal center is supported by a planar, tridentate pincer-coordinated bis(imino)pyridine ligand. The basic photophysical features of these compounds show significant elaboration in both number and intensity of the d–π* transitions observed in the UV/Vis spec tra relative to the bidentate starting materials, and these spectra were analyzed using time-dependent DFT computations. The redox nature of the bis(imino)pyridine ligand in compounds **2** and **4** was examined by electrochemical analysis, which showed two ligand reduction events and demonstrated that the ligand reduction shifts to a more positive potential when going from bidentate **2** to tridentate **4** (+160 mV for the first reduction step and +90 mV for the second). These observations indicate an increase in electrostatic stabilization of the reduced ligand in the tridentate conformation. Elaboration on this synthetic methodology documented its generality through the preparation of the pseudo-octahedral rhenium(I) triflate complex [(2,6-{2,6-$Me_2C_6H_3N{=}CPh\}_2C_5H_3N$)$Re(CO)_2$OTf] (**7**, 93 % yield).

Keywords: carbonyl ligands · non-innocent ligands · rhenium · solid-state reactions · tridentate ligands

Introduction

Although the element was discovered less than ninety years ago, the expanse of rhenium chemistry is impressive, with impact in the fields of catalysis,[1] fundamental photophysical properties,[2] and radiopharmaceuticals.[3] For example, the attractive photochemical and photophysical properties of α-diimine Re^I have attracted a great deal of attention since the mid-1970s, with pseudo-octahedral *fac*-$[ReX(CO)_3L_2]$ and *fac*-$[Re(CO)_3L_2(L')]^+$ complexes being the dominant species.[4] This large family of compounds is readily prepared by the addition of chelating σ-donor ligands to $[ReX(CO)_5]$ with the quantitative replacement of two *cis* carbonyl ligands in the Re^I starting material.[5] It is both interesting and significant that the formation of bidentate coordination to facial tricarbonyl isomers are the only reported products even when a potentially tridentate σ-donor is employed in the reaction (for example, **A** and **B**).[6,7] These robust species

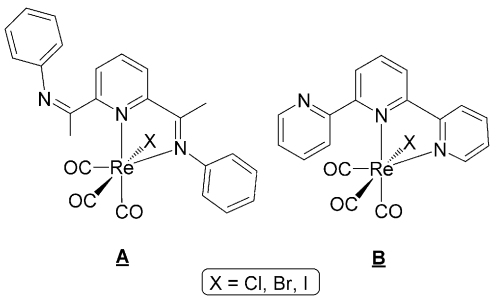

have been implicated for applications in organic light-emitting diodes (OLEDs),[8] chemosensors and biotechnology probes,[9] fluorescence microscopy imaging of cells,[10] and the photochemical reduction of CO_2 to CO.[11] Furthermore, the compact and robust rhenium tricarbonyl core is also a

[a] Dr. T. Jurca, S. Michel, Dr. I. Korobkov, Dr. D. S. Richeson
Centre for Catalysis Research and Innovation and
Department of Chemistry, University of Ottawa
Ottawa, Ontario, K1N 6N5 (Canada)
Fax: (+1) 613-562-5170
E-mail: darrin@uottawa.ca

[b] Dr. W.-C. Chen, Dr. T.-G. Ong
Institute of Chemistry Academia Sinica
Taipei, 115 (Taiwan)

Supporting information for this article is available on the WWW under http://dx.doi.org/10.1002/chem.201203045.

promising organometallic fragment for the labeling of biomolecules and in the development of diagnostic and therapeutic radiopharmaceuticals. Among the key photophysical features of the α-diimine Re^{I} compounds is the electron transfer capability of this system and the interplay between the Re center and the well-known non-innocent redox-activity of the ligands.

The bis(imino) pyridine family of ligands, pioneered by Brookhart and co-workers[12] and Gibson and co-workers[13] in base-metal olefin polymerization catalysis, present an interesting redox non-innocent ligand scaffold. While commonly employed as a neutral species, this ligand is stable in several chemically accessible reduced states represented by mono-, di-, or trianionic forms. The mono- and trianions are odd-electron, π radical species, in contrast to the dianionic state, which can be in a singlet or a triplet, unpaired ground state.[14]

Clearly the full potential of this versatile ligand scaffold cannot be exploited with the current, mature state of the chemistry of the *fac*-$[ReX(CO)_3L_2]$ owing to the limits imposed by the bidentate coordination. Furthermore, it would appear that, on the basis of the tridentate ligands that have been investigated, the concerted efforts to produce the tridentate species has been unsuccessful. Attracted by this challenge we sought to synthesize, crystallographically authenticate, and instigate investigation of the first low-valent rhenium pincer complex displaying an *N*,*N*′,*N*-chelated bis(imino)pyridine array. This report for the unconventional but accessible synthesis of tridentate pincer complexes promises to enhance the versatile chemistry of Re^{I} and yield new venues for exploration.

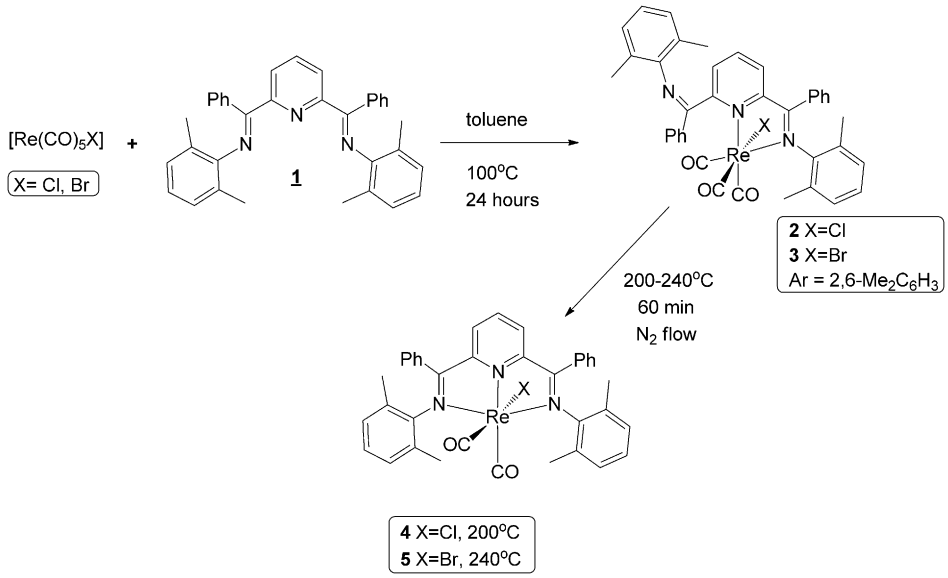

Scheme 1. Synthesis of tridentate pincer complexes **4** and **5**.

Results and Discussion

In a sealed reaction flask under N_2 atmosphere, the bis(imino)pyridine ligand **1** was allowed to react with 1 equivalent of $[Re(CO)_5X]$ (X = Cl or Br) as the reaction mixture was heated to 100 °C for 24 h (Scheme 1). The resulting bright red/orange powders were isolated in yields of 85% and 97%, respectively. While microanalysis provided the formulae of these two compounds and ^{1}H and ^{13}C NMR spectroscopy suggested their structural features, we were also successful in obtaining the detailed metrical parameters from single-crystal X-ray analyses for both products (Table 1). The two products, $[(2,6\text{-}\{2,6\text{-}Me_2C_6H_3N{=}CPh\}_2C_5H_3N)Re(CO)_3Cl]$ (**2**) and $[(2,6\text{-}\{2,6\text{-}Me_2C_6H_3N{=}CPh\}_2C_5H_3N)Re(CO)_3Br]$ (**3**) exhibited analogous ligand dispositions with the Re^{I} center in an octahedral geometry, as represented in Figure 1 and Figure 2. Selected bond distances and angles for **2** and **3** are presented in Table 2. As expected, the ligand coordinates in a bidentate mode through the pyridine nitrogen (N2) and one of the imine nitrogen atoms (N1). The second imine N-center (N3) is not coordinated to Re. The three carbonyl groups are facially oriented, a feature consistent with the observation of three IR bands for the CO stretches.[3b,4,15] The coordination geometries of these two compounds is completed by the re-

Table 1. Summary of data collection and crystallographic parameters for **2** and **3**.

Compound	**2**	**3**
empirical formula	$[C_{38}H_{31}ReClN_3O_3]$ $[C_4H_8O]$	$[C_{38}H_{31}ReBrN_3O_3]$ $[C_4H_8O]_{0.5}$
formula weight	871.41	879.82
T [K]	200(2)	296(2)
λ [Å]	0.71073	0.71073
crystal system	triclinic	triclinic
space group	$P\bar{1}$	$P\bar{1}$
a [Å]	8.4994(3)	9.645(3)
b [Å]	13.6344(4)	13.366(4)
c [Å]	16.6194(5)	15.955(5)
α [°]	102.8350(10)	107.958(13)
β [°]	97.3350(10)	99.607(15)
γ [°]	93.202(2)	90.663(14)
V [Å^3]	1855.36(10)	1924.7(11)
Z	2	2
ρ (calcd) [Mg m^{-3}]	1.560	1.518
μ [mm^{-1}]	3.393	4.235
asbsorption correction:	semi-empirical from equivalents	
final R indices [$I>2\sigma(I)$]		
$R1$[a]	0.0667	0.0201
$wR2$[b]	0.1285	0.0513

[a] $R1 = \sum \|F_o| - |F_c\| / \sum |F_o|$. [b] $wR2 = \left(\sum w(|F_o| - |F_c|)^2 / \sum w|F_o|^2\right)^{1/2}$.

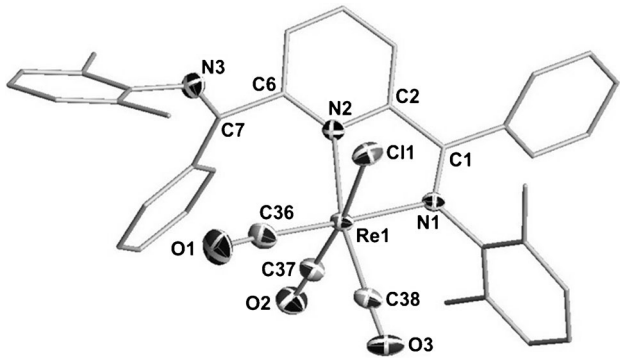

Figure 1. X-ray structure of compound **2**. Hydrogen atoms and co-crystallized THF omitted for clarity; ellipsoids set at 50% probability.

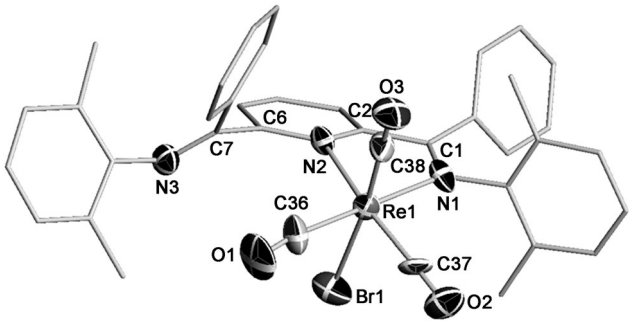

Figure 2. X-ray structure of compound **3**. Hydrogen atoms and co-crystallized THF omitted for clarity; ellipsoids set at 50% probability.

spective chloro or bromo groups that are *trans* to a carbonyl ligand and on an axis perpendicular to the plane of the coordinated nitrogen ligand.

Having compounds **2** and **3** in hand, our goal was to transform these species, through release of CO and coordination of the pendant imine group, into tridentate pincer ligand compounds and thus define a new coordination environment for Re^{I} carbonyl chemistry. With this in mind a computational analysis of the loss of CO and subsequent rearrangement of the pendant imine group to form a pincer type geometry, as shown in Scheme 1, was performed with DFT calculations using the Gaussian 09 suite of programs.[16] Frequency analysis on the optimized structures, using the B3LYP functional and mixed TZVP/LanL2DZ basis set, confirmed that these structures were minima and provided the data for the calculation of free energy (ΔG) and enthalpy (ΔH) of the reaction. Both of these values were positive ($\Delta G = 11.5$ kcal mol^{-1} and $\Delta H = 21.5$ kcal mol^{-1}). Combining this information with the fact that the entropy is a favorable, positive value, we successfully exploited this entropy-driven reaction by heating powders of **2** or **3** in a tube furnace under a dynamic flow of nitrogen. With this method and heating to 200 °C, compound **2** was transformed into a dark brown powder corresponding to a 97% yield of **4**. The symmetrical ^{1}H and ^{13}C NMR spectra, the appearance of only two CO stretches in the IR spectrum, and a satisfactory microanalysis confirmed the identity of this new species, and

Table 2. Selected bond lengths [Å] and angles [°] for compounds **2** and **3**.

2		**3**	
bond lengths:			
C1–C2	1.481(3)	C1–C2	1.46(2)
C6–C7	1.511(3)	C6–C7	1.49(2)
C1–N1	1.297(2)	C1–N1	1.303(18)
C7–N3	1.276(3)	C7–N3	1.285(18)
C2–N2	1.368(2)	C2–N2	1.376(18)
C6–N2	1.339(3)	C6–N2	1.350(18)
Re1–N1	2.1655(18)	Re1–N1	2.171(12)
Re1–N2	2.2200(15)	Re1–N2	2.249(12)
Re1–Cl1	2.4778(6)	Re1–Br1	2.623(2)
Re1–C36	1.930(2)	Re1–C36	1.93(2)
Re1–C37	1.905(2)	Re1–C37	1.907(17)
Re1–C38	1.900(2)	Re1–C38	1.91(2)
C36–O1	1.142(3)	C36–O1	1.127(18)
C37–O2	1.152(3)	C37–O2	1.152(17)
C38–O3	1.156(3)	C38–O3	1.135(18)
angles:			
N3-C7-C6	112.93(19)	N3-C7-C6	110.6(14)
C7-C6-N2	121.67(16)	C7-C6-N2	121.1(14)
C6-N2-Re1	128.01(13)	C6-N2-Re1	127.8(10)
N1-Re1-N2	74.69(6)	N1-Re1-N2	74.9(5)
N1-C1-C2	116.07(17)	N1-C1-C2	116.4(13)
C1-C2-N2	116.43(15)	C1-C2-N2	117.3(13)
C6-N2-C2	117.76(16)	C6-N2-C2	118.0(12)
Re1-N1-C1	118.37(14)	Re1-N1-C1	117.5(11)
Re1-N2-C2	113.43(12)	Re1-N2-C2	110.5(9)
N2-Re1-C36	105.41(8)	N2-Re1-C36	103.2(6)
N2-Re1-C38	167.22(8)	N2-Re1-C37	167.4(6)
N2-Re1-C37	96.45(8)	N2-Re1-C38	97.3(6)
N2-Re1-Cl1	80.48(5)	N2-Re1-Br1	81.4(3)
N1-Re1-C36	174.41(9)	N1-Re1-C36	177.1(7)
N1-Re1-C38	92.63(8)	N1-Re1-C37	94.2(6)
N1-Re1-C37	97.89(8)	N1-Re1-C38	95.1(6)
N1-Re1-Cl1	87.45(5)	N1-Re1-Br1	90.4(3)

definitive structural features of **4** were obtained by single-crystal X-ray analysis (Table 3). Along with the structural representation in Figure 3, selected bond distances and angles for **4** are presented in Table 4.

The Re^{I} center in the octahedral complex [(2,6-{2,6-$Me_2C_6H_3N{=}CPh\}_2C_5H_3N$)$Re(CO)_2Cl$] **4** is supported by a planar, pincer-coordinated bis(imino)pyridine ligand defined by the pyridine center (N2) and the imine nitrogen atoms

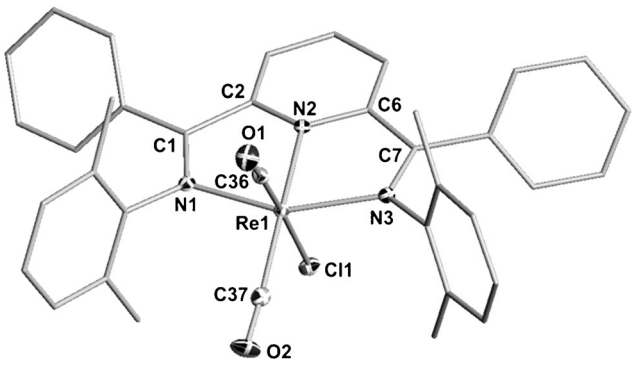

Figure 3. X-ray structure of compound **4**. Hydrogen atoms and THF omitted for clarity; ellipsoids set at 50% probability.

Table 3. Summary of data collection and crystallographic parameters for **4**.

Compound	**4**
empirical formula	$[C_{37}H_{31}ReClN_3O_2]\ [C_4H_8O]_{1.5}$
formula weight	879.45
T [K]	296(2)
λ [Å]	0.71073
crystal system	monoclinic
space group	$P2_1/n$
a [Å]	9.2686(3)
b [Å]	18.1949(6)
c [Å]	22.0310(7)
α [°]	90.00
β [°]	98.035(2)
γ [°]	90.00
V [Å^3]	3678.9(2)
Z	4
ρ (calcd) [Mg m^{-3}]	1.588
μ [mm^{-1}]	3.422
absorption correction:	semi-empirical from equivalents
final R indices [$I>2\sigma(I)$]	
$R1$[a]	0.0170
$wR2$[b]	0.0407

[a] $R1=\sum \|\|F_o\|-\|F_c\|\|/\sum|F_o|$. [b] $wR2=\left(\sum w(|F_o|-|F_c|)^2/\sum w|F_o|^2\right)^{1/2}$.

Table 4. Selected bond lengths [Å] and angles [°] for compound **4**.

4	
bond lengths:	
C1–C2	1.474(3)
C6–C7	1.477(3)
C1–N1	1.315(3)
C7–N3	1.309(3)
C2–N2	1.355(2)
C6–N2	1.353(2)
Re1–N1	2.0964(15)
Re1–N2	2.0672(16)
Re1–N3	2.1089(16)
Re1–Cl1	2.4751(5)
Re1–C36	1.897(2)
Re1–C37	1.914(2)
C36–O1	1.160(3)
C37–O2	1.158(3)
angles:	
N1-C1-C2	115.30(16)
N3-C7-C6	115.88(17)
C1-C2-N2	112.38(16)
C7-C6-N2	112.56(17)
C2-N2-C6	121.51(16)
C2-N2-Re1	118.18(13)
C6-N2-Re1	117.92(12)
N1-Re1-N2	75.79(6)
N3-Re1-N2	75.95(6)
N1-Re1-N3	151.72(6)
N2-Re1-C37	170.88(7)
N2-Re1-C36	105.01(7)
N2-Re1-Cl1	79.67(4)

(N1, and N3). One of the carbonyl groups lies in this plane and *trans* to the pyridyl group. The remaining CO (C36) and chloro ligands are perpendicular to this plane and define the axial sites. The Re–N pyridine distance of 2.0672(16) Å is slightly shorter than the Re–N imine distances of 2.0964(15) Å and 2.1089(16) Å; these bond lengths are significantly shorter than those observed for bidentate complex **2**, indicating a stronger ligand–metal interaction. The remaining metal ligand distances are similar to those observed in **2**.

To achieve a complete transformation of bidentate **3** to the pincer complex **5**, an increased temperature of 240 °C and a reaction time of 1 hour were required. Once again this procedure led to the isolation of dark brown powder of **5** in 95 % yield. The ^{1}H and ^{13}C NMR, IR spectroscopic similarities to **4**, and also the microanalysis of this compound confirmed its identity as the octahedral Re^{I} complex [(2,6-{2,6-$Me_2C_6H_3N$=CPh}$_2C_5H_3N$)Re(CO)$_2$Br] **5**. However, crystals suitable for X-ray crystallography could not be obtained.

UV/Vis and electrochemical characterization: The deeper color of **4** compared to **2** is evident in the UV/Vis spectra of these species and is presented in Figure 4. These spectra were obtained in acetonitrile with identical concentrations

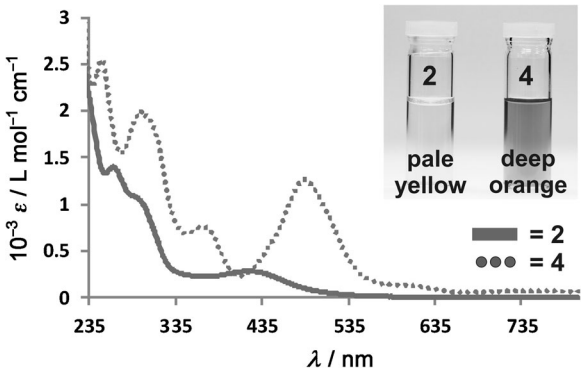

Figure 4. UV/Vis spectra of compound **2** (bidentate) and **4** (tridentate) in acetonitrile (concentration = 0.08 mM).

of 0.08 mM. The most obvious differences between the two species involve the d–π* transitions in the 350–550 nm region of the spectrum. The higher-energy bands are ligand based π–π* transitions. Bidentate ligated 2 has a broad signal at 419 nm, while tridentate species **4** has more intense signals at 367 and 485 nm, which are likely to be responsible for the color change observed (see inset in Figure 4).

These UV/Vis spectra were modeled in acetonitrile solution using time-dependent DFT computations with Gaussian 09 software, the B3LYP functional, mixed TZVP/LanL2DZ basis set, and the PCM solvent model.[17] The resulting computed spectra were excellent matches to the experimental spectra, and are shown in Supporting Information, Figures S1 and S2. In the case of compound **2**, the observed 419 nm (23 900 cm^{-1}) absorbance consists of two equal intensity electronic transitions centered at 440 nm (22 700 cm^{-1}) and 392 nm (22 500 cm^{-1}). The computations reveal that the 440 nm contribution is a transition from the HOMO−2, rhenium-centered d level to the LUMO that is a ligand-based π* orbital (d–π*), while the 395 nm component

is a ligand-based π–π* transition. In contrast, the two distinctive transitions at 485 nm (20600 cm^{-1}) and 367 nm (27250 cm^{-1}) for tridentate species **4** are both d–π* transitions. The computational model provided a large absorbance transition at 458 nm (21800 cm^{-1}) that was made up of equal contributions from three d–π* transitions that involve electronic transitions from three different rhenium d-orbital levels to ligand π* orbitals. The computations also provided a band at 368 nm (27200 cm^{-1}) that corresponds to a d–π* transition.

The redox-non-innocent nature of the bis(imino)pyridine ligation was examined using cyclic voltammetry on the free ligand and of both the bi- and tridentate species. Cyclic voltammograms (CV) of **1**, **2**, and **4** reveal quasi-reversible reduction waves (Figure 5). The CV of **1** reveals only one

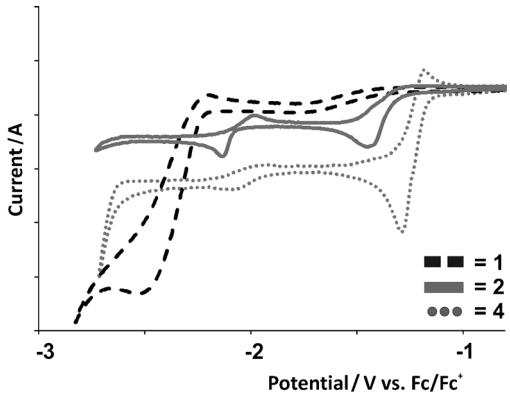

Figure 5. Cyclic voltammograms in acetonitrile of free bis(imino)pyridine ligand **1**, and complexes **2** and **4** referenced to the ferrocene/ferrocenium cation couple.

quasi-reversible reduction within the window afforded by acetonitrile. This signal corresponds to the established formation of the bis(imino)pyridine monoanion. The quasi-reversiblility of all of these reductions is supported by the fact that they exhibit a ΔE_p greater than that of the reversible one-electron ferrocene/ferrocenium couple (ΔE_p for Fc/Fc^+ = 80 mV) used as a reference, as well as cathodic currents that are smaller than the anodic reduction currents. For **2** and **4**, the waves are assigned as successive one-electron reductions of the bis(imino)pyridine ligand within the respective rhenium complex. Formation of ML^{2-} species is not uncommon for bis(imino)pyridines, which have been shown to facilitate the formation of mono-, di-, and trianionic complexes.[14] The reduction behavior of compound **2** is similar to the electrochemical behavior that has been noted previously for related aromatic N-donor ligand systems (diimine- and pyridine-based).[14h,18,19] No oxidation waves were observed within the solvent window.

Bidentate complex **2** has two quasi-reversible reduction waves with cathodic maxima at −1.45 V and −2.13 V ($E_{1/2}$ = −2.07 V, ΔE_p = 140 mV) versus the Fc/Fc^+ couple. Tridentate complex **4** presented a similar pattern, with cathodic maxima at −1.29 V ($E_{1/2}$ = −1.25 V, ΔE_p = 106 mV) and −2.04 V ($E_{1/2}$ = −1.98 V, ΔE_p = 130 mV). We attribute the quasi-reversible nature of the first reduction wave to a chemical transformation of this first reduction product, $[\mathbf{2}]^-$ or $[\mathbf{4}]^-$.[18] The smaller current observed for the second reduction wave was ascribed to this transformation and concomitant decrease in concentration of these species. The first reduction wave for both compounds have similar values to those reported for coordinated bis(imino)pyridine ligands and the potential separation between the two redox processes (680 mV for **2** and 750 mV for **4**) is a typical value for aromatic N-donor ligands bound to rhenium(I).[18] The drastic difference in potentials between the first reduction in **2** and **4** (−1.45 and −1.29 V respectively), and that of free ligand **1** (−2.52 V, $E_{1/2}$ = −2.36 V) illustrates the electrostatic stabilization of the reduced forms of the ligand by the rhenium(I) cation. Furthermore, the shift to less-negative potential when going from bidentate **2** to tridentate **4** (+160 mV for the first reduction step and +90 mV for the second) indicates an increase in electrostatic stabilization of the reduced ligand in the tridentate conformation. This is not surprising as ligand–metal contact has increased from two to three N-donor interactions.

Synthesis of a triflate analogue: Activation of the Re−X moiety is an initial fundamental feature for exploration of the reactivity of these new species, and exchange of chloride by triflate, which is known to be a more labile anion, was chosen to begin this examination. Reaction of **4** with a slight excess of AgOTf resulted in the isolation of a mixture of dark brown and purple powder. Unfortunately, despite our efforts, we have so far been unable to isolate significant quantities of these products to carry out further analysis. As direct halide abstraction from **4** did not lead to clean product formation, an alternative route to formation of the targeted triflate complex was applied. As outlined in Scheme 2, the direct synthesis of the triflate complex **6** was targeted with subsequent solid-state conversion to the desired pincer geometry.

Reaction of **2** with a slight excess of AgOTf resulted in the isolation of bright yellow/orange powder in a moderate yield. While the spectroscopic features were consistent with the proposed formulation, X-ray analysis (Table 5) confirmed the product to be the octahedral Re^I complex [(2,6-{2,6-$Me_2C_6H_3N$=CPh}$_2C_5H_3N$)Re(CO)$_3$(OTf)] **7** (Figure 6). Selected bond lengths and angles for **7** are presented in Table 6. Complex **7** is the analogue of compound **2** and **3** with halide replaced by a triflate anion.

Compound **6** could be converted cleanly into the tridentate species **7** by heating a powder sample to 190 °C under a flow of nitrogen for 25 min. The resulting dark brown powder was confirmed to be [(2,6-{2,6-$Me_2C_6H_3N$=CPh}$_2C_5H_3N$)Re(CO)$_2$(OTf)] **7** by spectroscopic characterization, microanalysis, and X-ray structural analysis.

Figure 7 shows the results of the structural examination (Table 5), with selected bond distances and angles for presented in Table 6. These data confirm this complex to be the octahedral Re^I complex [(2,6-{2,6-$Me_2C_6H_3N$=CPh}$_2C_5H_3N$)-

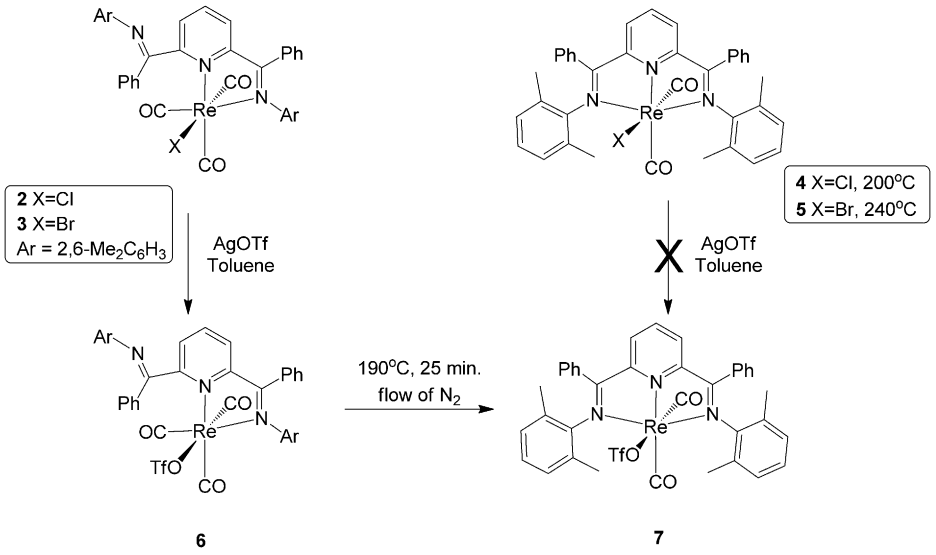

Scheme 2. Synthesis of the tridentate triflate complex **7**.

Table 5. Summary of data collection and crystallographic parameters for **6** and **7**.

Compound	**6**	**7**
empirical	$[C_{38}H_{31}Re(CF_3SO_3)N_3O_3]$	$[C_{37}H_{31}Re(CF_3SO_3)N_3O_3]$
formula	$[C_4H_8O]$	$[CHCl_3]$
formula weight	985.03	1004.29
T [K]	200(2)	200(2)
λ [Å]	0.71073	0.71073
crystal system	triclinic	triclinic
space group	$P\bar{1}$	$P\bar{1}$
a [Å]	8.6739(2)	13.8597(11)
b [Å]	12.3727(3)	15.6045(11)
c [Å]	19.2872(4)	18.8333(14)
α [°]	87.8370(10)	81.639(4)
β [°]	83.6820(10)	84.582(4)
γ [°]	76.1410(10)	78.114(4)
V [Å^3]	1997.29(8)	3934.7(5)
Z	2	4
ρ (calcd) [Mg m^{-3}]	1.638	1.695
μ [mm^{-1}]	3.163	3.407
absorption correction:	semi-empirical from equivalents	
final R indices $[I>2\sigma(I)]$		
$R1$[a]	0.0298	0.0814
$wR2$[b]	0.0602	0.1921

[a] $R1=\sum||F_o|-|F_c||/\sum|F_o|$. [b] $wR2=\left(\sum w(|F_o|-|F_c|)^2/\sum w|F_o|^2\right)^{1/2}$.

$Re(CO)_2(OTf)]$ **7**.[20] This transformation involved loss of CO *trans* to the coordinated imine moiety with rearrangement of the non-coordinated imine side-arm to afford the desired pincer ligand geometry that was isolated in 93% yield with no further workup. The geometry around the Re^I center is similar to that of compound **4** with an OTf^- anion replacing the chloro ligand and a plane defined by the pyridine center (N2), imine nitrogen atoms (N1 and N3), and a CO carbon atom (C37). The axial sites are defined by a CO carbon (C36) and a triflate oxygen (O3). IR stretches for the carbonyl group at 1915 and 1855 cm^{-1} are similar to those observed in **4** and **5**. The preparative route to **7** demonstrates the generality of the thermal synthesis approach.

Conclusion

We have reported the first crystallographically authenticated low-valent rhenium pincer complexes and have thus addressed a major deficiency in the chemistry of imine-coordinated Re^I carbonyl chemistry. This family of compounds was accessed through an unconventional but highly efficient solid-state thermolysis synthetic route and they possess a redox active non-innocent tridentate bis-

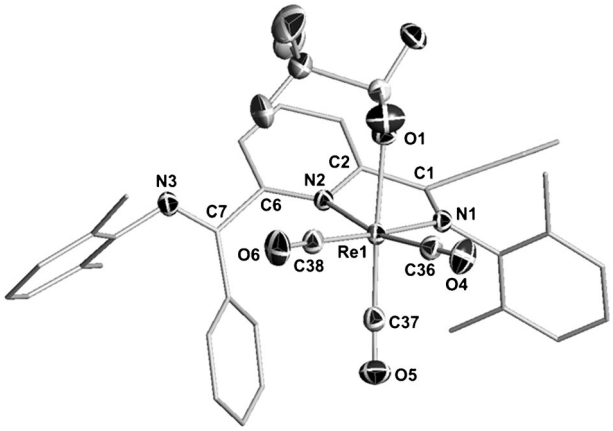

Figure 6. X-ray structure of compound **6**. Hydrogen atoms and THF omitted for clarity; ellipsoids set at 50% probability.

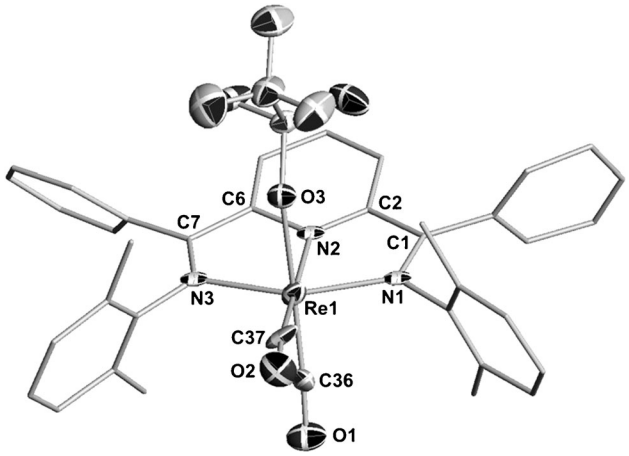

Figure 7. X-ray structure of compound **7**. Hydrogen atoms, $CHCl_3$, and THF omitted for clarity; ellipsoids set at 50% probability.

Table 6. Selected bond lengths [Å] and angles [°] for compounds **6** and **7**.

6		**7**	
bond lengths:			
C1–C2	1.489(4)	C1–C2	1.54(3)
C6–C7	1.505(4)	C6–C7	1.47(3)
C1–N1	1.288(4)	C1–N1	1.37(3)
C7–N3	1.275(4)	C7–N3	1.30(3)
C2–N2	1.364(4)	C2–N2	1.27(3)
C6–N2	1.348(4)	C6–N2	1.44(3)
Re1–N1	2.154(2)	Re1–N1	2.073(16)
Re1–N2	2.228(2)	Re1–N2	2.028(17)
Re1–O1	2.200(2)	Re1–N3	2.136(17)
Re1–C36	1.908(3)	Re1–O3	2.198(13)
Re1–C37	1.882(3)	Re1–C36	1.86(2)
Re1–C38	1.923(3)	Re1–C37	1.87(3)
C36–O4	1.150(4)	C36–O1	1.18(3)
C37–O5	1.162(4)	C37–O2	1.21(3)
C38–O6	1.146(4)		
angles:			
N3-C7-C6	114.2(3)	N1-C1-C2	112(2)
C7-C6-N2	121.4(3)	N3-C7-C6	116(2)
C6-N2-Re1	128.3(2)	C1-C2-N2	109(2)
N1-Re1-N2	74.23(9)	C7-C6-N2	113(2)
N1-C1-C2	115.6(3)	C2-N2-C6	117(2)
C1-C2-N2	114.5(3)	C2-N2-Re1	125.8(17)
C6-N2-C2	117.2(3)	C6-N2-Re1	116.7(14)
Re1-N1-C1	117.38(19)	N1-Re1-N2	74.2(7)
Re1-N2-C2	109.69(18)	N3-Re1-N2	77.4(7)
N2-Re1-C38	101.32(11)	N1-Re1-N3	151.6(7)
N2-Re1-C36	168.19(11)	N2-Re1-C37	170.2(8)
N2-Re1-C37	103.58(12)	N2-Re1-C36	103.1(9)
N2-Re1-O1	76.06(8)	N2-Re1-O3	81.8(6)
N1-Re1-C38	175.43(11)		
N1-Re1-C36	99.01(11)		
N1-Re1-C37	93.94(12)		
N1-Re1-O1	82.23(8)		

(imino)pyridine chelate. While known α-diimine Re^{I} compounds display very interesting and useful photophysical and redox features, the newly reported contributions to this family, reported herein, expand on these characteristics. Specifically, these new pincer complexes display enhanced metal-to-ligand d–π* electronic transitions both in number and intensity. DFT analysis allowed a detailed understanding for these transitions. Furthermore, there are some clear modifications to the redox chemistry provided by this newly obtained tridentate ligation. The shift of the reduction potentials to less negative values for the tridentate system indicated an increase in electrostatic stabilization of the reduced ligand in the tridentate conformation. Furthermore, an efficient route to generate bis(imino)pyridine Re^{I} pincer complexes bearing the weakly bound triflate anion should facilitate future reactivity studies and potential catalytic applications. The substantially enhanced features of these new species as well as the clear future avenues for steric and electronic modifications promise to amplify the versatile chemistry of Re^{I} and yield new avenues for exploration.

Experimental Section

General methods: Reactions were performed in a glovebox with a nitrogen atmosphere. Solvents were sparged with nitrogen and then dried by passage through a column of activated alumina using an apparatus purchased from Anhydrous Engineering. Deuterated chloroform was dried using activated molecular sieves. Rhenium starting materials were purchased from Strem Chemicals and used as received. All other chemicals were purchased from Aldrich and used without further purification. NMR spectra were run on Bruker Avance 300 and 500 MHz spectrometers with $CDCl_3$ as solvent and internal standard. Bis(imino)pyridine ligand (**1**) was synthesized according to literature procedure.[21] Elemental analyses for **2**–**7** were performed by Midwest Microlab LLC, Indianapolis IN. Solid state reactions were carried out in a Lindberg Blue M Mini-Mite Tube Furnace (model TF55035A-1). Infrared spectra were collected using a Varian 640 FTIR spectrometer using an ATR attachment.

Electrochemical measurements: Electrochemical measurements were performed with a Princeton Applied Research (PAR) 2273 potentiostat/galvanostat running Power Suite 2.58 electrochemical software using a one-compartment three-electrode cell. Platinum wire working and counter electrodes, a silver wire pseudo-reference electrode, and 0.1 M tetrabutylammonium bromide (Sigma Aldrich, 99.0%) in acetonitrile (Fisher Scientific, 99.9%) as supporting electrolyte were employed; ferrocene was added as an internal standard at the end of each experiment. The electrochemical cell was degassed with nitrogen prior to measurement. Cyclic voltammograms of 5 mM **1**, **3**, and **4** were recorded at 50 $mV s^{-1}$. A nitrogen environment was maintained in the cell throughout all of the measurements.

[(2,6-{2,6-$Me_2C_6H_3N$=CPh}$_2C_5H_3N$)Re(CO)$_3$Cl] (2): $[Re(CO)_5Cl]$ powder (68 mg, 0.190 mmol) was added to a clear yellow solution of **1** (100 mg, 0.203 mmol) in toluene (8 mL), in which $[Re(CO)_5Cl]$ remained insoluble. The reaction mixture was placed in a Teflon-sealed flask and allowed to stir at 100 °C for 24 h, over which time a bright orange precipitate formed. The solution was filtered, the precipitate was washed with of hexanes (5×2 mL), and allowed to dry under vacuum. A bright red/orange powder was isolated in 97% yield. Large red plate-like crystals suitable for X-ray analysis were grown from a saturated solution of THF with hexanes, and storing at −20 °C for several days. $\tilde{\nu}$(CO) = 2013 (s), 1918 (s), 1896 cm^{-1} (s). ^{1}H NMR ($CDCl_3$, 500 MHz): δ = 8.21 (br d, 1H, py, aromatic), 8.09 (br t, 1H, py, aromatic), 7.59 (br d, 1H, aromatic), 7.45–6.83 (br m, 16H, aromatic), 6.80 (br d, 1H, aromatic), 2.60 (br s, 3H, Me), 2.41 (br s, 3H, Me), 1.99 (br s, 3H, Me), 1.71 ppm (br s, 3H, Me). ^{13}C NMR ($CDCl_3$, 125 MHz). δ = 196.3 (CO), 195.1 (CO), 186.0 (CO), 178.1 (C=N imine), 163.9 (py, C=N imine), 162.8 (o-C=N), 157.7 (o-C=N), 148.3 (Ar, *i*-C), 147.2 (Ar, *i*-C), 139.2 (Ar-CH), 133.4 (Ar, *i*-C), 133.1 (Ar, C-CH_3), 131.4 (Ar-CH), 131.1 (Ar-CH), 131.0 (Ar, C-CH3), 130.9 (Ar-CH), 130.5 (Ar-CH), 130.0 (Ar-CH), 128.8 (Ar-CH), 128.7 (Ar-CH), 128.6 (Ar-CH), 128.4 (Ar-CH), 128.2 (Ar-CH), 128.1 (Ar-CH), 127.7 (Ar-CH), 126.9 (Ar-CH), 126.2 (Ar, C-CH_3), 123.9 (Ar-CH), 122.8 (Ar, C-CH_3), 20.3 (Ar-Me, CH_3), 18.7 (br, Ar-Me, CH_3), 18.4 ppm (Ar-Me, CH_3). Elemental analysis calcd (%) for [$C_{38}H_{31}ReClN_3O_3$]: C 57.10, H 3.91, N 5.26; found: C 57.48, H 3.92, N 5.38.

[(2,6-{2,6-$Me_2C_6H_3N$=CPh}$_2C_5H_3N$)Re(CO)$_3$Br] (3): $[Re(CO)_5Br]$ powder (95 mg, 0.234 mmol) was added to a clear yellow solution of **1** (150 mg, 0.305 mmol) in toluene (8 mL), in which $[Re(CO)_5Br]$ remained insoluble. The reaction mixture was placed in a Teflon-sealed flask and allowed to stir at 100 °C for 24 h, over which time a bright red/orange precipitate formed. The solution was filtered, the precipitate was washed with hexanes (5×2 mL), and allowed to dry under vacuum. A bright red/orange powder was isolated in 85% yield. Large red plate-like crystals suitable for X-ray analysis were grown from a saturated solution of THF with hexanes, and storing at −20 °C for several days. $\tilde{\nu}$(CO) = 2024 (s), 1932 (s), 1897 cm^{-1} (s). ^{1}H NMR ($CDCl_3$, 500 MHz): δ = 8.24 (br d, 1H, py, aromatic), 8.09 (br t, 1H, py, aromatic), 7.62 (br d, 1H, aromatic), 7.47–6.88 (br m, 15H, aromatic) 6.84 (br d, 1H, aromatic), 6.80 (br d, 1H, aromatic), 2.65 (br s, 3H, Me), 2.44 (br s, 3H, Me), 1.96 (br s, 3H, Me), 1.66 ppm (br s, 3H, Me). ^{13}C NMR ($CDCl_3$, 125 MHz). δ = 195.7 (CO), 194.9 (CO), 185.3 (CO), 177.9 (C=N imine), 163.9 (py, C=N imine), 163.0

(*o*-C=N), 157.9 (*o*-C=N), 148.5 (Ar, *i*-C), 147.1 (Ar, *i*-C), 139.1 (Ar-CH), 133.3 (Ar, *i*-C), 133.2 (Ar, C-CH_3), 131.3 (Ar-CH), 131.1 (Ar-CH), 131.0 (Ar-CH), 130.9 (Ar, C-CH_3), 130.5 (Ar-CH), 129.2 (Ar-CH), 128.7 (Ar-CH), 128.7 (Ar-CH), 128.6 (Ar-CH), 128.5 (Ar-CH), 128.4 (Ar-CH), 128.3 (Ar-CH), 128.2 (Ar-CH), 128.1 (Ar-CH), 127.8 (Ar-CH), 126.1 (Ar, C-CH_3), 123.9 (Ar-CH), 122.5 (Ar, C-CH_3), 21.1 (Ar-Me, CH_3), 18.7 (Ar-Me, CH_3), 18.6 (Ar-Me, CH_3), 18.4 ppm (Ar-Me, CH_3). Elemental analysis calcd (%) for $[C_{38}H_{31}ReBrN_3O_3]$: C 53.90, H 4.05, N 4.96; found: C 54.01, H 3.93, N 5.05.

[(2,6-{2,6-$Me_2C_6H_3N$=CPh}$_2C_5H_3N$)Re(CO)$_2$Cl] (4): A powder sample of **2** (120 mg, 0.149 mmol) was placed in a ceramic boat inside a quartz tube under flow of N_2 and placed inside a furnace. The reaction was allowed to run for 1 hour at 200 °C, after which the boat was removed and allowed to cool. A dark brown/red powder was isolated in 97% yield. Small dark brown prism-like crystals suitable for X-ray analysis were grown from a saturated solution of THF with hexanes, and after storing at −20 °C for several days. $\tilde{\nu}$(CO) = 1919 (s), 1849 cm^{-1} (s). ^{1}H NMR ($CDCl_3$, 500 MHz): δ = 7.66 (brd, 2H, py, *m*-CH), 7.42 (brt, 2H, aromatic), 7.33 (brt, 2H, aromatic), 7.16 (brt, 2H, aromatic), 7.07 (brm, 3H, aromatic), 7.01 (brd, 2H, aromatic), 6.96 (brd, 2H, aromatic), 6.81 (brt, 2H, aromatic), 6.70 (brd, 2H, aromatic), 2.76 (brs, 6H, Me), 2.12 ppm (brs, 6H, Me). ^{13}C NMR ($CDCl_3$, 125 MHz). δ = 221.8 (CO), 174.6 (C=N imine), 166.2 (CO), 161.8 (py, *o*-C=N), 151.2 (Ar, *i*-C), 138.1 (Ar-CH), 132.5 (Ar, *i*-C), 132.1 (Ar, *i*-C), 130.9 (Ar-CH), 130.0 (Ar-CH), 128.8 (Ar-CH), 128.6 (Ar-CH), 128.5 (Ar-CH), 128.3 (Ar-CH), 128.2 (Ar-CH), 127.9 (Ar-CH), 127.8 (Ar-CH), 126.8 (Ar, *i*-C), 126.2 (Ar-CH), 124.4 (Ar-CH), 20.2 (Ar-Me, CH_3), 19.1 ppm (Ar-Me, CH_3). Elemental analysis calcd (%) for $[C_{37}H_{31}ReClN_3O_3]$: C 57.61, H 4.05, N 5.45: found: C 57.43, H 4.03, N 5.44.

[(2,6-{2,6-$Me_2C_6H_3N$=CPh}$_2C_5H_3N$)Re(CO)$_2$Br] (5): A powder sample of **3** (60 mg, 0.071 mmol) was placed in a ceramic boat inside a quartz tube under flow of N_2 and placed inside a furnace. The reaction was allowed to run for 1 hour at 240 °C, after which the boat was removed and allowed to cool. A dark brown/red powder was isolated in 95% yield. Small dark prism-like crystals were grown from a variety of solvents (ether, THF, chloroform) but were consistently too small and unsuitable for X-ray analysis. $\tilde{\nu}$(CO) = 1906 (s), 1837 cm^{-1} (s). ^{1}H NMR ($CDCl_3$, 500 MHz): δ = 7.66 (brm, 2H, py, aromatic), 7.49–6.88 (brm, 13H, aromatic), 6.83 (brt, 2H, aromatic), 6.72 (brd, 2H, aromatic), 2.82 (brs, 6H, Me), 2.14 ppm (brs, 6H, Me). ^{13}C NMR ($CDCl_3$, 125 MHz). δ = 221.6 (vbr CO), 174.9 (C=N imine), 167.1 (CO), 161.9 (py, *o*-C=N), 151.8 (Ar, *i*-C), 138.4 (Ar-CH), 133.1 (Ar, *i*-C), 132.3 (Ar, *i*-C), 131.3 (Ar-CH), 130.4 (Ar-CH), 129.2 (Ar-CH), 128.9 (Ar-CH), 128.6 (Ar-CH), 128.4 (Ar-CH), 128.2 (Ar-CH), 127.1 (Ar, *i*-C), 126.6 (Ar-CH), 124.6 (Ar-CH), 21.7 (Ar-Me, CH_3), 19.6 ppm (Ar-Me, CH_3). Elemental analysis calcd (%) for $[C_{37}H_{31}ReBrN_3O_3]$: C 54.48, H 3.83, N 5.15; found: C 53.94, H 3.78, N 5.09.

[(2,6-{2,6-$Me_2C_6H_3N$=CPh}$_2C_5H_3N$)Re(CO)$_3$(CF_3SO_3)] (6): A powder sample of **2** (150 mg, 0.187 mmol) and slight excess of AgOTf (51 mg, 0.200 mmol) were added to toluene (8 mL) in a darkened reaction flask. The reaction mixture was allowed to stir for 18 h, over which time a bright yellow precipitate formed. The solution was filtered, the solid was washed with hexanes (5 × 2 mL) then dissolved in dichloromethane and filtered through a plug of Celite. This solution was then concentrated under vacuum. A bright yellow powder was isolated in 55% yield. Yellow plate-like crystals suitable for X-ray analysis were grown from a saturated solution of THF with hexanes, and storing at −20 °C for several days. $\tilde{\nu}$(CO) = 2030 (s), 1931 (s), 1912 cm^{-1} (s). ^{1}H NMR ($CDCl_3$, 500 MHz): δ = 8.21 (brd, 1H, py, aromatic), 8.42 (brd, 1H, py, aromatic), 8.19 (brt, 1H, aromatic), 7.65 (brd, 1H, aromatic), 7.45 (brt, 1H, aromatic), 7.37 (brm, 2H, aromatic), 7.32 (brm, 2H, aromatic), 7.28–7.11 (brm, 4H, aromatic), 7.03 (brm, 3H, aromatic), 6.93 (brt, 2H, aromatic), 6.84 (brd, 1H, aromatic), 6.77 (brd, 1H, aromatic), 2.49 (brs, 3H, Me), 2.38 (brs, 3H, Me), 2.02 (brs, 3H, Me), 1.52 ppm (brs, 3H, Me). ^{13}C NMR ($CDCl_3$, 125 MHz). δ = 195.9 (CO), 194.6 (CO), 187.4 (CO), 179.6 (C=N imine), 163.7 (py, C=N imine), 163.3 (*o*-C=N), 157.5 (*o*-C=N), 147.4 (Ar, *i*-C), 147.2 (Ar, *i*-C), 140.3 (Ar-CH), 133.4 (Ar, *i*-C), 132.4 (Ar, C-CH_3), 131.9 (Ar-CH), 131.4 (Ar-CH), 131.3 (Ar-CH), 130.7 (Ar-CH), 130.5 (Ar, C-CH_3), 130.1 (Ar, C-CH_3), 129.5 (Ar-CH), 128.9 (Ar-CH), 128.8 (Ar-CH), 128.7 (Ar-CH), 128.4 (Ar-CH), 128.0 (Ar-CH), 127.7 (Ar-CH), 127.2 (Ar-CH), 126.2 (Ar, C-CH_3), 124.2 (Ar-CH), 18.8 (Ar-Me, CH_3), 18.4 (Ar-Me, CH_3), 18.3 (Ar-Me, CH_3), 18.2 ppm (Ar-Me, CH_3). A sample for elemental analysis was obtained by recrystallization in $CHCl_3$, resulting in a 1:1 $CHCl_3$ adduct of **7** calcd (%) for $[C_{39}H_{31}F_3N_3O_6ReS][CHCl_3]$: C 46.54, H 3.12, N 4.07; found: C 46.85, H 3.22, N 4.22.

[(2,6-{2,6-$Me_2C_6H_3N$=CPh}$_2C_5H_3N$)Re(CO)$_2$(CF_3SO_3)] (7): A powder sample of **6** (50 mg, 0.055 mmol) was placed in a ceramic boat, inside a quartz tube under flow of N_2 and placed inside a furnace. The reaction was allowed to run for 25 min at 190 °C, after which the boat was removed and allowed to cool. A dark brown/red powder was isolated in 93% yield. Small orange plate-like crystals suitable for X-ray analysis were grown in a saturated solution of $CHCl_3$ with hexanes, and storing at −20 °C for several days. $\tilde{\nu}$(CO) = 1915 (s), 1855 cm^{-1} (s). ^{1}H NMR ($CDCl_3$, 500 MHz): δ = 7.59 (brd, 2H, py, *m*-CH), 7.49–6.99 (brm, 13H, aromatic), 6.81 (brt, 2H, aromatic), 6.71 (brd, 2H, aromatic), 2.66 (brs, 6H, Me), 2.19 ppm (brs, 6H, Me). ^{13}C NMR ($CDCl_3$, 125 MHz). δ = 220.4 (CO), 178.9 (C=N imine), 169.1 (CO), 163.9(py, *o*-C=N), 150.4 (Ar, *i*-C), 140.7 (Ar-CH), 131.7 (Ar, *i*-C), 131.6 (Ar, *i*-C), 131.3 (Ar-CH), 129.4 (Ar-CH), 129.3 (Ar-CH), 128.9 (Ar-CH), 128.6 (Ar-CH), 128.3 (Ar-CH), 128.2 (Ar-CH), 127.3 (Ar-CH), 126.7 (Ar, *i*-C), 126.6 (Ar-CH), 126.4 (Ar-CH), 19.4 (Ar-Me, CH_3), 19.0 ppm (Ar-Me, CH_3). Elemental analysis calcd (%) for $[C_{38}H_{31}F_3N_3O_5ReS]$: C 51.58, H 3.53, N 4.75; found: C 51.31, H 3.44, N 4.80.

Acknowledgements

We thank the Natural Sciences and Engineering Research Council (NSERC) of Canada for funding.

[1] a) B. Dudle, K. Rajesh, O. Blacque, H. Berke, *J. Am. Chem. Soc.* **2011**, *133*, 8168; b) K. R. Jain, W. A. Herrmann, F. E. Kühn, *Coord. Chem. Rev.* **2008**, *252*, 556; c) Y. Kuninobu, K. Takai, *Chem. Rev.* **2011**, *111*, 1938.

[2] M. P. Coogan, V. Fernández-Moreira, B. M. Kariuki, S. J. A. Pope, F. L. Thorp-Greenwood, *Angew. Chem.* **2009**, *121*, 5065; *Angew. Chem. Int. Ed.* **2009**, *48*, 4965.

[3] a) M. Bartholomä, J. Valliant, K. P. Maresca, J. Babich, J. Zubieta, *Chem. Commun.* **2009**, 493; b) R. Schibli, P. A. Schubiger, *Eur. J. Nucl. Med.* **2002**, *29*, 1529.

[4] a) S. M. Fredericks, J. C. Luong, M. S. Wrighton, *J. Am. Chem. Soc.* **1979**, *101*, 7415; b) L. Sacksteder, A. P. Zipp, E. A. Brown, J. Streich, J. N. Demas, *Inorg. Chem.* **1990**, *29*, 4335; c) G. Ruiz, E. Wolcan, M. R. Féliz, *J. Photochem. Photobiol. A* **1996**, *101*, 119; d) M. R. Feliz, F. Rodriguez-Nieto, G. Ruiz, E. Wolcan, *J. Photochem. Photobiol. A* **1998**, *117*, 185; e) V. W.-W. Yam, *Chem. Commun.* **2001**, 789; f) J. V. Caspar, T. J. Meyer, *J. Phys. Chem.* **1983**, *87*, 952; g) R. Lin, Y. Fu, C. P. Brock, T. F. Guarr, *Inorg. Chem.* **1992**, *31*, 4346; h) J. K. Hino, L. Dellaciana, W. J. Dressick, B. P. Sullivan, *Inorg. Chem.* **1992**, *31*, 1072; i) K. A. Walters, Y.-J. Kim, J. T. Hupp, *Inorg. Chem.* **2002**, *41*, 2909; j) D. R. Striplin, G. A. Crosby, *Coord. Chem. Rev.* **2001**, *211*, 163.

[5] For some examples, see a) T. A. Martin, C. E. Ellul, M. F. Mahon, M. E. Warren, D. Allan, M. K. Whittlesey, *Organometallics* **2011**, *30*, 2200; b) E. W. Abel, G. Wilkinson, *J. Chem. Soc.* **1959**, 1501; c) W. J. Kirkham, A. G. Osborne, R. S. Nyholm, M. H. B. Stiddard, *J. Chem. Soc.* **1965**, 550; d) F. Zingales, U. Sartorelli, A. Trovati, *Inorg. Chem.* **1967**, *6*, 1246; e) F. Zingales, M. Graziani, F. Faraone, U. Belluco, *Inorg. Chim. Acta* **1967**, *1*, 172; f) D. R. Gamelin, M. W. George, P. Glyn, F.-W. Grevels, F. P. A. Johnson, W. Klotzbücher, S. L. Morrison, G. Russell, K. Schaffner, J. J. Turner, *Inorg. Chem.* **1994**, *33*, 3246; g) A. A. Martí, G. Mezei, L. Maldonado, G. Paralitici, R. G. Raptus, J. L. Colón, *Eur. J. Inorg. Chem.* **2005**, 118; h) M. Wrighton,

D. L. Morse, *J. Am. Chem. Soc.* **1974**, *96*, 998; i) P. J. Giordano, S. M. Fredericks, M. S. Wrighton, D. L. Morse, *J. Am. Chem. Soc.* **1978**, *100*, 2257; j) P. J. Giordano, M. S. Wrighton, *J. Am. Chem. Soc.* **1979**, *101*, 2888.

[6] a) K. G. Orrell, A. G. Osborne, V. Sik, M. W. daSilva, M. B. Hursthouse, D. E. Hibbs, K. M. A. Malik, N. G. Vassilev, *J. Organomet. Chem.* **1997**, *538*, 171; b) J. Granifo, S. J. Bird, K. G. Orrell, A. G. Osborne, V. Sik, *Inorg. Chim. Acta* **1999**, *295*, 56.

[7] E. W. Abel, V. S. Dimitrov, N. J. Long, K. G. Orrell, A. G. Osborne, H. M. Pain, V. Sik, M. B. Hursthouse, M. A. Mazid, *J. Chem. Soc. Dalton Trans.* **1993**, 597.

[8] X. Gong, P. K. Ng, W. K. Chan, *Adv. Mater.* **1998**, *10*, 1337.

[9] a) K. K. W. Lo, M. W. Louie, K. Y. Zhang, *Coord. Chem. Rev.* **2010**, *254*, 2603; b) T. P. Lin, C. Y. Chen, Y. S. Wen, S. S. Sun, *Inorg. Chem.* **2007**, *46*, 9201; c) R. V. Slone, D. I. Yoon, R. M. Calhoun, J. T. Hupp, *J. Am. Chem. Soc.* **1995**, *117*, 11813; d) P. D. Beer, V. Timoshenko, M. Maestri, P. Passaniti, V. Balzani, *Chem. Commun.* **1999**, 1755; e) P. D. Beer, E. J. Hayes, *Coord. Chem. Rev.* **2003**, *240*, 167.

[10] a) A. J. Amoroso, M. P. Coogan, J. E. Dunne, V. Fernandez-Moreira, J. B. Hess, A. J. Hayes, D. Lloyd, C. Millet, S. J. A. Pope, C. Williams, *Chem. Commun.* **2007**, 3066; b) K. K.-W. Lo, M. Louie, K. Sze, J. Lau, *Inorg. Chem.* **2008**, *47*, 602; c) A. J. Amoroso, R. J. Arthur, M. P. Coogan, J. B. Court, V. Fernandez-Moreira, A. J. Hayes, D. Lloyd, C. Millet, S. J. A. Pope, *New J. Chem.* **2008**, *32*, 1097.

[11] a) J. Hawecker, J. M. Lehn, R. Ziessel, *J. Chem. Soc. Chem. Commun.* **1983**, 536; b) O. Ishitani, M. W. George, T. Ibusuki, F. P. A. Johnson, K. Koike, K. Nozaki, C. Pac, J. J. Tumer, J. R. Westwell, *Inorg. Chem.* **1994**, *33*, 4712; c) P. Christensen, A. Hamnet, A. V. G. Muir, J. A. Timney, *J. Chem. Soc. Dalton Trans.* **1992**, 1455; d) B. P. Sullivan, C. M. Bolinger, D. Conrad, W. J. Vining, T. J. Meyer, *J. Chem. Soc. Chem. Commun.* **1985**, 1414.

[12] B. L. Small, M. Brookhart, *J. Am. Chem. Soc.* **1998**, *120*, 7143.

[13] G. J. P. Britovsek, V. C. Gibson, B. S. Kimberley, P. J. Maddox, S. J. McTavish, G. A. Solan, A. J. P. White, D. J. Williams, *Chem. Commun.* **1998**, 849.

[14] The ability of bis(imino)pyridine ligands to take on negative charge, thereby behaving as radical species is well documented: a) D. Zhu, P. H. M. Budzelaar, *Organometallics* **2008**, *27*, 2699; b) J. Scott, S. Gambarotta, I. Korobkov, Q. Knijnenburg, B. de Bruin, P. H. M. Budzelaar, *J. Am. Chem. Soc.* **2005**, *127*, 17204; c) A. M. Archer, M. W. Bouwkamp, M. P. Cortez, E. Lobkovsky, P. J. Chirik, *Organometallics* **2006**, *25*, 4269; d) T. Jurca, K. Dawson, I. Mallov, T. Burchell, G. P. A. Yap, D. S. Richeson, *Dalton Trans.* **2010**, *39*, 1266; e) P. J. Chirik, K. Wieghardt, *Science* **2010**, *327*, 794; f) K. G. Caulton, *Eur. J. Inorg. Chem.* **2012**, 435; g) Q. Knijnenburg, S. Gambarotta, P. H. M. Budzelaar, *Dalton Trans.* **2006**, 5442; h) P. H. M. Budzelaar, B. de Bruin, A. W. Gal, K. Wieghardt, J. H. van Lenthe, *Inorg. Chem.* **2001**, *40*, 4649; i) B. de Bruin, E. Bill, E. Bothe, T. Weyhermüller, K. Wieghardt, *Inorg. Chem.* **2000**, *39*, 2936; j) S. C. Bart, K. Chlopek, E. Bill, M. W. Bouwkamp, E. Lobkovsky, F. Neese, K. Wieghardt, P. J. Chirik, *J. Am. Chem. Soc.* **2006**, *128*, 13901.

[15] M. Schutte, G. Kemp, H. Visser, A. Roodt, *Inorg. Chem.* **2011**, *50*, 12486.

[16] Gaussian 09 (Revision A.1), M. J. Frisch, G. W. Trucks, H. B. Schlegel, G. E. Scuseria, M. A. Robb, J. R. Cheeseman, G. Scalmani, V. Barone, B. Mennucci, G. A. Petersson, H. Nakatsuji, M. Caricato, X. Li, H. P. Hratchian, A. F. Izmaylov, J. Bloino, G. Zheng, J. L. Sonnenberg, M. Hada, M. Ehara, K. Toyota, R. Fukuda, J. Hasegawa, M. Ishida, T. Nakajima, Y. Honda, O. Kitao, H. Nakai, T. Vreven, J. A. Montgomery, Jr., J. E. Peralta, F. Ogliaro, M. Bearpark, J. J. Heyd, E. Brothers, K. N. Kudin, V. N. Staroverov, R. Kobayashi, J. Normand, K. Raghavachari, A. Rendell, J. C. Burant, S. S. Iyengar, J. Tomasi, M. Cossi, N. Rega, J. M. Millam, M. Klene, J. E. Knox, J. B. Cross, V. Bakken, C. Adamo, J. Jaramillo, R. Gomperts, R. E. Stratmann, O. Yazyev, A. J. Austin, R. Cammi, C. Pomelli, J. W. Ochterski, R. L. Martin, K. Morokuma, V. G. Zakrzewski, G. A. Voth, P. Salvador, J. J. Dannenberg, S. Dapprich, A. D. Daniels, Ö. Farkas, J. B. Foresman, J. V. Ortiz, J. Cioslowski, D. J. Fox, Gaussian, Inc., Wallingford CT, **2009**.

[17] Details are provided in the Supporting Information.

[18] a) F. Paolucci, M. Marcaccio, C. Paradisi, S. Roffia, C. A. Bignozzi, C. Amatore, *J. Phys. Chem. B* **1998**, *102*, 4759; b) G. J. Stor, F. Hartl, J. W. van Outersterp, D. J. Stufkens, *Organometallics* **1995**, *14*, 1115; c) M. S. Jana, A. K. Pramanik, S. Kundu, T. K. Mondal, *Polyhedron* **2012**, *40*, 46; B. D. Rossenaar, F. Hartl, D. J. Stufkens, *Inorg. Chem.* **1996**, *35*, 6194.

[19] The LUMO and LUMO+1 molecular orbitals for both compounds **2** and **4** are ligand-centered and π^* in nature. See the Supporting Information, Figures S3 and S4 for representations of these orbitals.

[20] Higher temperatures or prolonged reaction results in decomposition. The powder turns black and there is a multitude of unassignable peaks in the ^{1}H NMR.

[21] T. Jurca, I. Korobkov, G. P. A. Yap, S. I. Gorelsky, D. S. Richeson, *Inorg. Chem.* **2010**, *49*, 10635.

Received: August 28, 2012
Revised: November 15, 2012
Published online: February 1, 2013

